A novel coupled physics-based electromagnetic model of semiconductor traveling-wave structures for RF and optoelectronic applications

F. Bertazzi, F. Cappelluti, F. Bonani, M. Goano, G. Ghione

Politecnico di Torino, Dipartimento di Elettronica and CERCOM,
Corso Duca degli Abruzzi 24, I-10129 Torino, Italy, Phone +39 011 564 4140

Abstract— **The design of traveling-wave structures for high-speed analog and digital circuits requires accurate modeling to deal with arbitrary cross-sections, metallic regions with finite conductivity, and semiconductor layers. The presence of such high-conductivity layers can strongly affect the microwave propagation characteristics of quasi-TEM transmission lines; in fact, free carrier screening of the electric field in regions penetrated by the magnetic field can lead to slow-wave behaviour. In the present paper, we present a numerical technique which combines a charge transport model with the quasi-static solution of Maxwell's equations, thus allowing an accurate and self-consistent evaluation of the quasi-TEM line parameters. The proposed approach is applied to the analysis of a Si-Ge p-i-n traveling-wave photodetector.**

I. Introduction

The design of microwave, millimeter-wave and optoelectronic circuits on semiconductor substrates requires the accurate characterization of complex waveguiding structures. The presence of high-conductivity layers can strongly affect the propagation characteristics of the microwave line. In the low frequency range (often extending, in integrated structures, up to mm-waves) the electric field is usually confined in low-doping regions, whereas the magnetic field extends deep into doped layers. The partial spatial separation of the fields leads to a larger capacitance and a smaller inductance. As a result, the structure exhibits a significant decrease in the microwave phase velocity. Such a slow-wave propagation has been both experimentally and theoretically analyzed in metal-insulator-semiconductor (MIS) lines [1]. In the slow-wave propagation regime the microwave effective index may be much larger than the value expected from the relative dielectric constants of any of the substrate layers. This may also lead to serious problems in the design of optoelectronic traveling wave structures where syncronous coupling with an optical signal is required.

In the present paper, we focus on the interaction mechanisms between the electromagnetic field and the charged carriers in the semiconductor. In order to describe the field-carriers interaction in semiconducting materials, a transport model is included in the electromagnetic simulation.

In [2] a coupled physics-based electromagnetic model has been proposed for the three-dimensional analysis of interconnet structures. In [3], a quasi-static integral spectral domain analysis is proposed for the analysis of multistrips on layered insulator-semiconductor substrates. Recently, a full-wave technique incorporating the semiconductor transport model and Maxwell's equations has been introduced [4].

In many applications, however (e.g. passive transmission lines for high-speed digital or analog integrated circuits, distributed travelling-wave optoelectronic and electronic devices) the size reduction of the device cross-section makes modal dispersion virtually negligible for quasi-TEM propagation on a wide frequency range; in such cases, the quasi-static FEM model is a viable alternative to the full-wave analysis. This suggests that a quasi-static, quasi-TEM transmission-line approach can be conveniently exploited in coupling the semiconductor transport model to Maxwell's equations in a consistent way, with obvious computational advantages and little loss of accuracy.

Among the solution techniques to EM problems allowing for anisotropic materials, conductor and dielectric losses, and arbitrary (e.g. nonplanar) geometries, the finite-element method (FEM) is probably the most flexible and powerful. In the present paper, we extend the quasi-static finite-element technique introduced in [5], [6] to combine the solution of Maxwell's equations with a charge transport model. The proposed approach exploits existing techniques to obtain the small-signal solution of the 2D transport problem in the device cross-section, and compute self-consistently the small-signal conduction current along the propagation direction according to a magneto-quasi-static model [5]. The present formulation leads to the definition of the per-unit-length (p.u.l.) series impedance and parallel admittance, respectively, of the microwave line in small-signal operation. A nonlinear model of the line is currently under investigation.

The present numerical technique is applied to the analysis of a traveling-wave photodetector (TW-PD) with a Si-Ge p-i-n structure. The results have been compared with full-wave finite-element computations [7] obtained assuming fixed carrier distributions and describing semiconductor layers with a uniform conductivity model. The device-level simulation shows that the electromagnetic analysis of traveling-wave structures on semiconductor substrates indeed requires the inclusion of carrier transport into the electromagnetic model.

II. Small-signal model

Consider a microwave transmission line consisting of metal conductors embedded in a lossy, non-homogeneous dielectric-semiconductor medium characterized by the complex permittivity constant ϵ. Dielectric losses in insulators are included in the small-signal model through a frequency-dependent loss angle. Let us assume that the line is uniform along the z-axis, and let the electrodes have arbitrary cross-sections and finite conductivity σ.

The small cross-sectional dimensions of high-speed interconnects suggest the validity of quasi-TM (approximately quasi-TEM, the longitudinal component of the electric field originating from losses) modal propagation. In this approach, the longitudinal component of the magnetic field is assumed as negligible. With these assumptions, the electric field and the relevant transversal components of the magnetic field may be obtained from a scalar magnetic potential A and an electric potential ϕ [8]:

$$\mathbf{B} = -\hat{z} \times \nabla_t A \tag{1}$$

$$\mathbf{E} = -\nabla_t \phi - (\partial\phi/\partial z)\hat{z} - (\partial A/\partial t)\hat{z}. \tag{2}$$

We assume also that the transverse electric field in the conductors is negligible, whereas in the same regions a small z-component of the electric field exists, related to the conduction current density J_z.

With these approximations, the electric and magnetic problems can be decoupled, thus leading to the separate evaluation of the transverse magnetic and electric fields, respectively. The transverse E-field outside the conductors is computed through a conventional drift-diffusion physics-based model. The transverse H-field is then evaluated through a magneto-quasi-static formulation, which computes the longitudinal current density self-consistently with the drift-diffusion solution in the transverse plane. The two formulations immediately lead to the definition of the p.u.l. series impedance and parallel admittance, respectively, of the microwave line.

A. Transverse E-field formulation

The electrostatic potential ϕ must satisfy the Poisson equation:

$$-\nabla_t \cdot (\epsilon \nabla_t \phi) = q\,(N_D^+ - N_A^- + p - n) \tag{3}$$

where N_D^+, N_A^- are the ionized donor and acceptor densities in the semiconsuctor layers, and n and p are electron and hole concentrations, respectively. In (3), ϕ is assumed constant over the metal conductors: the transverse components of the electric field are considered negligible inside the electrodes. The electron and hole concentrations must satisfy the continuity equations:

$$\partial n/\partial t - 1/q(\nabla_t \cdot \mathbf{J}_n) + U_n = 0 \tag{4}$$

$$\partial p/\partial t + 1/q(\nabla_t \cdot \mathbf{J}_p) + U_p = 0. \tag{5}$$

The constitutive equations that relate the transversal currents to the electric field and the carrier densities are expressed as the sum of a drift and a diffusion term:

$$\mathbf{J}_n = -qn\mu_n \nabla_t \phi + qD_n \nabla_t n \tag{6}$$

$$\mathbf{J}_p = -qp\mu_p \nabla_t \phi - qD_p \nabla_t p \tag{7}$$

where μ_α and D_α ($\alpha = n, p$) are the field-dependent mobilities and diffusivities, respectively, U_n and U_p are the net recombination rates for electrons and holes. Equations (3), (4) and (5) are solved according to the Scharfetter-Gummel discretization scheme in order to avoid spurious spatial oscillations [9]. In DC conditions, time derivatives in (4) and (5) can be set to zero and the resulting system of nonlinear equations can be solved through the Newton method. After the device has been DC biased, small-signal excitations can be analyzed by direct linearization around the DC working point and transformation into the frequency domain:

$$-\nabla_t \cdot (\epsilon \nabla_t \phi_{ss}) = q\,(p_{ss} - n_{ss}) \tag{8}$$

$$j\omega n_{ss} + \nabla_t \cdot (n_0\mu_n \nabla_t \phi_{ss} + n_{ss}\mu_n \nabla_t \phi_0 - D_n \nabla_t n_{ss}) + U_n = 0 \tag{9}$$

$$j\omega p_{ss} - \nabla_t \cdot (n_0\mu_p \nabla_t \phi_{ss} + p_{ss}\mu_p \nabla_t \phi_0 + D_p \nabla_t p_{ss}) + U_p = 0 \tag{10}$$

where n_0 and p_0 are the electron and hole concentrations at the bias point, ϕ_{ss} is the small-signal component of ϕ, and n_{ss}, p_{ss} are the small-signal electron and hole concentrations. In the present model, mobilities μ_n and μ_p are assumed constant. Thermionic emission across abrupt heterojunction interfaces is included introducing suitable interface conditions [10]. Small-signal analysis is carried out at each frequency point in the range of interest. The small-signal p.u.l. parallel admittance $\mathcal{Y}(\omega) = G(\omega) + j\omega C(\omega)$ may then be obtained from the small-signal current entering the active contact.

B. Transverse H-field formulation

The magnetic potential A is not unique unless a gauge condition is imposed. Using the Lorentz condition

$$\partial A/\partial z = -j\omega\mu_0\epsilon\phi \tag{11}$$

an inhomogeneous Helmholtz equation for the magnetic potential A results [11]:

$$-\nabla_t^2 A - k_0^2 \epsilon_r A = \mu_0 J_z \tag{12}$$

where $k_0 = \omega\sqrt{\epsilon_0\mu_0}$ is the free-space wavenumber, and J_z is the total small-signal conduction current density. Neglecting displacement currents, equation (12) takes the form

$$-\nabla_t^2 A = \mu_0 J_z. \tag{13}$$

In the semiconductor layers, the z-directed current density J_z may be written as:

$$J_z = -j\omega(qn_0\mu_n + qp_0\mu_p)A - (qn_0\mu_n + qp_0\mu_p)\partial\phi_{ss}/\partial z + qD_n\,\partial n_{ss}/\partial z - qD_p\,\partial p_{ss}/\partial z. \tag{14}$$

Assuming the longitudinal dependence of the fields as $\exp(-j\gamma z)$, with $\gamma = \beta - j\alpha$ being the complex propagation constant, and substituting (14) in (13), we have:

$$-\nabla_t^2 A + j\omega\mu_0(qn_0\mu_n + qp_0\mu_p)A = + j\mu_0(qn_0\mu_n + qp_0\mu_p)\gamma\phi_{ss} - j\mu_0 qD_n\gamma n_{ss} + \mu_0 qD_p\gamma p_{ss} \tag{15}$$

Inside conductive media Ohm's law holds:

$$-\nabla_t^2 A_{ss} + j\omega\mu_0\sigma A_{ss} = j\mu_0\sigma\gamma V_{ss} \tag{16}$$

where V_{ss} is the AC voltage applied to the metal conductor (boundary condition on ϕ_{ss} on the conductor surface) and σ is the metal conductivity. Finally,

$$\nabla_t^2 A_{ss} = 0 \tag{17}$$

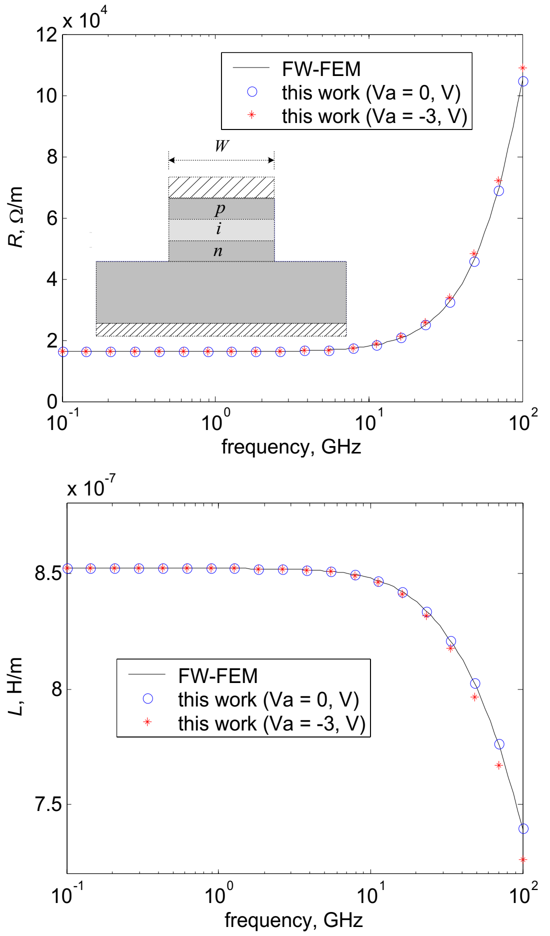

Fig. 1: Small-signal per-unit-length resistance and inductance computed vs. frequency with the full-wave finite-element technique (solid line) and with the current approach, at thermodynamic equilibrium (circles) and at the reverse bias voltage of 3 V (crosses).

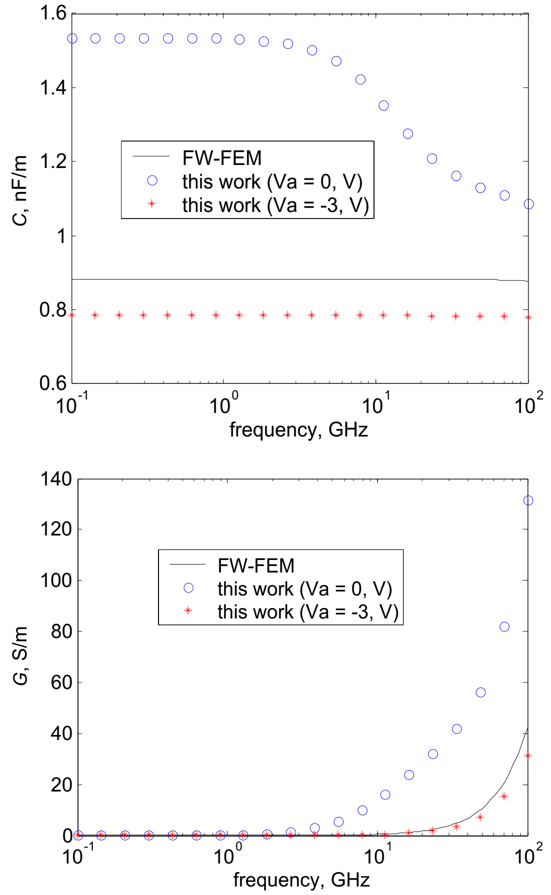

Fig. 2: Small-signal per-unit-length capacitance and conductance computed vs. frequency with the full-wave finite-element technique (solid line) and with the current approach, at thermodynamic equilibrium (circles) and at the reverse bias voltage of 3 V (crosses).

in insulator media, where currents are zero. The source current density distribution $J_{s,z}$ in (15) and (16) is known but for a constant factor, the complex propagation constant γ. We solve (15), (16) and (17) for A/γ. Notice that γ cancels out in the computation of the small-signal p.u.l. series impedance $\mathcal{Z}(\omega) = R(\omega) + j\omega L(\omega)$, which can be derived integrating the power loss density $E_z J^*_{s,z} = (j\gamma\phi_{ss} - j\omega A) J^*_{s,z}$. The present numerical technique computes the longitudinal currents self-consistently with the drift-diffusion solution in the transverse plane. Also, the penetration of the electromagnetic field in the metallic regions is rigorously computed, allowing for the accurate evaluation of conduction losses in any frequency range.

III. Case study

As an example, we consider a bulk Si-Ge TW-PD sketched in the inset of Fig. 1. The microwave structure of the device is a microstrip line (the gold electrode thickness is $t = 1\,\mu$m, the central electrode width is $W = 3\,\mu$m) on a ridge-type semiconductor substrate (the ridge height is $h = 2\,\mu$m). Doping levels for p- and n-type silicon are 10^{18} cm^{-3}, and the doping level of the n-type germanium active region is 10^{16} cm^{-3}. The p-type and intrinsic layer thicknesses are $h_p = 1\,\mu$m, $d = 0.5\,\mu$m, respectively.

The p.u.l. circuit parameters and the microwave propagation characteristics, without illumination, have been computed with the present technique at two bias points, see Figs. 1–4. The results have been compared with those obtained with a full-wave finite element approach [7], assuming the intrinsic layer as completely depleted. As expected, the p.u.l. series impedance does not depend on the bias voltage, since the active region has a negligible contribution to the longitudinal current. In contrast, the p.u.l. capacitance exhibit an appreciable frequency dispersion if the active layer is not completely depleted. The slow-wave structure shows strong microwave attenuation, because the electromagnetic field penetrates inside the doped semiconductor.

The optical power dependent photocurrent in travelling-wave optoelectronic devices can in some cases (e.g. in WT-EAMs, see the discussion in [12]) significantly affect the microwave properties at high optical powers by increasing the parallel conductance; in TW-PDs effects due to photogenerated carrier field screening are expected to arise only in saturation. The current photogenerated in the active region may be readily included in the model, introducing a carrier radiative generation term in the continuity equations (4), (5), as implemented in [13].

From the bias-dependent small-signal characterization, a nonlinear (in the electrical and optical variables) coupled RF-optical model can be readily extracted for the interaction structure. Such a model can be exploited within the framework of finite-difference time-domain approaches for

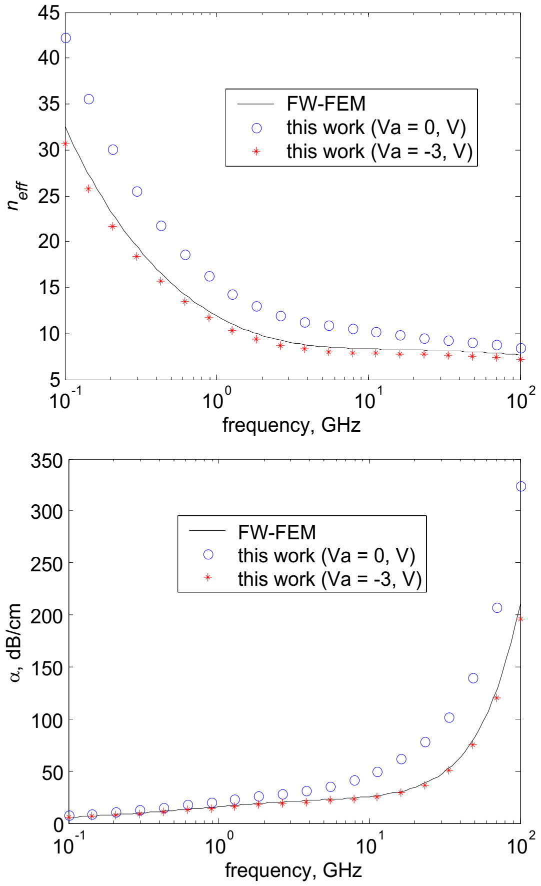

Fig. 3: Microwave effective index and attenuation constant computed vs. frequency with the full-wave finite-element technique (solid line) and with the current approach, at thermodynamic equilibrium (circles) and at the reverse bias voltage of 3 V (crosses).

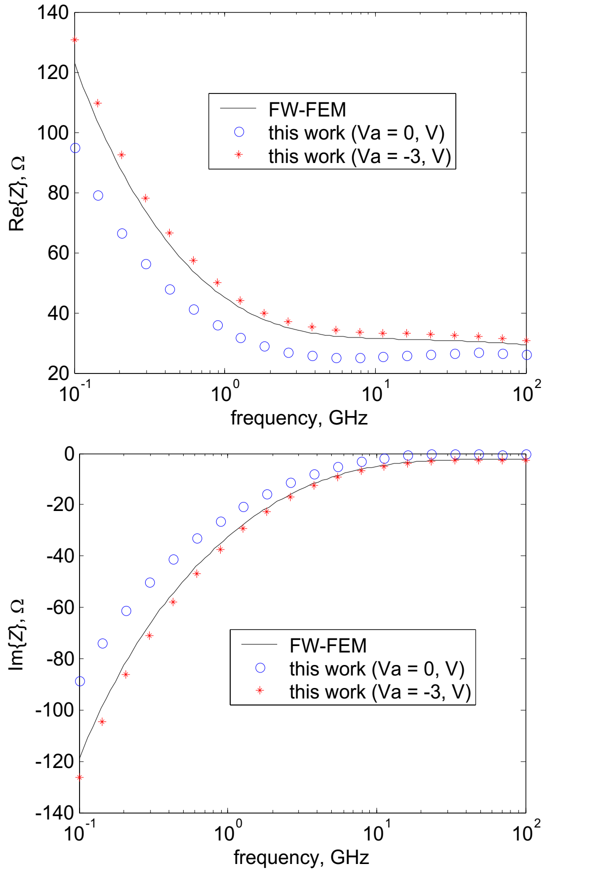

Fig. 4: Characteristic impedance computed vs. frequency with the full-wave finite-element technique (solid line) and with the current approach, at thermodynamic equilibrium (circles) and at the reverse bias voltage of 3 V (crosses).

nonlinear large-signal simulation [14], or of frequency-domain harmonic-balance techniques within an RF circuit simulation environment.

IV. Conclusion

We have presented a novel finite-element small-signal model for the analysis of distributed structures on semiconductor substrates. Maxwell's equations are solved self-consistently with the charge carrier transport in the semiconductor layers. The present approach enables to model field-carrier interactions, slow-wave propagation, external bias effects, and screening effects of the charged carriers. The simulation of a bulk travelling-wave Si-Ge photodetector demonstrates that the electromagnetic analysis of TW-PDs indeed requires the inclusion of carrier transport into the model.

References

[1] E.S. Tony and S. K. Chaudhuri, "Effect of depletion layer on the propgation characteristics of MIS transmission lines," *IEEE Trans. Microwave Theory Tech.*, vol. MTT-47, no. 9, pp. 1760–1763, Sept. 1999.

[2] P. Meuris, W. Schoenmaker, and W. Magnus, "Strategy for electromagnetic interconnect modeling," *IEEE Trans. Computer-Aided Design*, vol. CAD-20, no. 6, pp. 753–762, June 2001.

[3] J. Aguilera, R. Marques, and M. Horno, "Improved quasi-static spectral domain analysis of microstrip lines on high-conductivity insulator-semiconductor substrates," *IEEE Microwave Guided Wave Lett.*, vol. 9, no. 2, pp. 57–59, Feb. 1999.

[4] G. Wang, R. W. Dutton, and C. S. Rafferty, "Device-level simulation of wave propagation along metal-insulator-semiconductor interconnects," *IEEE Trans. Microwave Theory Tech.*, vol. MTT-50, no. 4, pp. 1127–1136, Apr. 2002.

[5] F. Bertazzi, F. Carbonera, M. Goano, and G. Ghione, "FEM-based reduced-order model for steady-state skin-effect analysis in lossy lines," in *IEEE MTT-S International Microwave Symposium*, Seattle, June 2002, pp. 2025–2028.

[6] F. Bertazzi, G. Ghione, and M. Goano, "Efficient quasi-TEM frequency-dependent analysis of lossy multiconductor lines through a fast reduced-order FEM model," *IEEE Trans. Microwave Theory Tech.*, accepted for publication.

[7] F. Bertazzi, O. A. Peverini, M. Goano, G. Ghione, R. Orta, and R. Tascone, "A fast reduced-order model for the full-wave FEM analysis of lossy inhomogeneous anisotropic waveguides," *IEEE Trans. Microwave Theory Tech.*, vol. MTT-50, no. 9, pp. 2108–2114, Sept. 2002.

[8] J. Aguilera, R. Marqués, and M. Horno, "Quasi-TEM surface impedance approaches for the analysis of MIC and MMIC transmission lines, including both conductor and substrate losses," *IEEE Trans. Microwave Theory Tech.*, vol. MTT-43, no. 7, pp. 1553–1558, July 1995.

[9] G. Ghione and A. Benvenuti, "Discretization schemes for high-frequency semiconductor device models," *IEEE Trans. Antennas Propagation*, vol. AP-45, no. 3, pp. 443–456, Mar. 1997.

[10] D. Schroeder, *Model of Interface Carrier Transport for Device Simulation*, Computational Microelectronics. Springer-Verlag, Wien, 1994.

[11] S. Ramo, J. R. Whinnery, and T. Van Duzer, *Fields and Waves in Communication Electronics*, Wiley, New York, 3rd edition, 1994.

[12] G. L. Li, C. K. Sun, S. A. Pappert, W. X. Chen, and P. K. L. Yu, "Ultrahigh-speed traveling-wave electroabsorption modulator–design and analysis," *IEEE Trans. Microwave Theory Tech.*, vol. MTT-47, no. 7, pp. 1177–1183, July 1999.

[13] D. Meglio, P. Lugli, R. Sabella, and O. Sahlén, "Analysis and optimization of InGaAsP electro-absorption modulators," *IEEE J. Quantum Electron.*, vol. QE-31, no. 2, pp. 261–268, Feb. 1995.

[14] F. Cappelluti and G. Ghione, "Self-consistent time-domain large-signal model of high-speed traveling-wave electroabsorption modulators," *IEEE Trans. Microwave Theory Tech.*, vol. MTT-51, no. 4, pp. 1096–1104, Apr. 2003.